

Micro- and nanoelectronics. Condensed matter physics  
Микро- и нанoeлектроника. Физика конденсированного состояния

UDC 538.958

<https://doi.org/10.32362/2500-316X-2024-12-2-57-66>

## RESEARCH ARTICLE

## Magnetorefractive effect in metallic Co/Pt nanostructures

Alexey N. Yurasov<sup>@</sup>,  
Diana A. Sayfullina,  
Tatiana N. Bakhvalova

MIREA – Russian Technological University, Moscow, 119454 Russia

<sup>@</sup> Corresponding author, e-mail: [alexey\\_yurasov@mail.ru](mailto:alexey_yurasov@mail.ru)

### Abstract

**Objectives.** To carry out a theoretical investigation of the features of magnetorefractive effect for metal-to-metal nanostructures. This study uses the example of multilayer Co/Pt nanostructures (ferromagnetic metal–paramagnetic metal) with a different ratio of ferromagnetic and paramagnetic phases in the visible and near-infrared (IR) spectral regions.

**Methods.** The dependence was expressed explicitly using the basic formulas for permittivity, refraction and extinction coefficients, and optical conductivity. This then confirms the common nature of these two effects. The magnetorefractive effect for s-polarization of light was calculated using Fresnel formulas for a three-layer structure. This took into account the thickness of the samples and the influence of the substrate. Effective medium methods were used to calculate the dielectric permittivity of materials. Since the average range of cobalt concentrations was being studied, the Bruggeman approximation was used to establish the effective permittivity of nanostructures. The reflection coefficient at normal incidence was calculated for all nanostructures.

**Results.** Since the permittivity of inhomogeneous samples was replaced by a common effective parameter depending on the permittivity of each component, we were able to apply the Drude–Lorentz theory for conductors in a high-frequency alternating field and then estimate the parameters of the electronic structure of the samples being studied. Plasma and relaxation frequencies were calculated for each sample. This made it possible for the number of free electrons to be estimated and scattering in nanostructures to be investigated.

**Conclusions.** It was shown that Langmuir shielding can be observed in the given energy range in the IR region of the spectrum. The calculated values correlate well with the experimental data.

**Keywords:** magnetorefractive effect, giant magnetoresistance, ferromagnet, nanostructures

• Submitted: 09.07.2023 • Revised: 06.10.2023 • Accepted: 12.02.2024

**For citation:** Yurasov A.N., Sayfullina D.A., Bakhvalova T.N. Magnetorefractive effect in metallic Co/Pt nanostructures. *Russ. Technol. J.* 2024;12(2):57–66. <https://doi.org/10.32362/2500-316X-2024-12-2-57-66>

**Financial disclosure:** The authors have no a financial or property interest in any material or method mentioned.

The authors declare no conflicts of interest.

НАУЧНАЯ СТАТЬЯ

## Магниторефрактивный эффект в металлических наноструктурах Co/Pt

А.Н. Юрасов<sup>®</sup>,  
Д.А. Сайфулина,  
Т.Н. Бахвалова

МИРЭА – Российский технологический университет, Москва, 119454 Россия

<sup>®</sup> Автор для переписки, e-mail: alexey\_yurasov@mail.ru

### Резюме

**Цели.** Теоретически исследовать особенности магниторефрактивного эффекта для наноструктур типа металл – металл на примере многослойных наноструктур Co/Pt (ферромагнитный металл – парамагнитный металл) с разным соотношением ферромагнитной и парамагнитной фаз в видимой и ближней инфракрасной (ИК) областях спектра.

**Методы.** С помощью основных формул для диэлектрической проницаемости, оптической проводимости, коэффициентов рефракции и экстинкции, выявлена и выражена в явном виде связь магниторефрактивного эффекта с эффектом гигантского магнитосопротивления (магниторезистивным эффектом), что подтверждает общую природу этих двух эффектов. С помощью формул Френеля для трехслойной структуры рассчитан магниторефрактивный эффект для s-поляризации света с учетом толщины образцов и влияния подложки. Для расчета диэлектрической проницаемости материалов применялись методы эффективной среды. Так как исследовался средний диапазон концентраций кобальта, то для нахождения эффективных диэлектрических проницаемостей наноструктур применялось приближение Бруггемана. Для всех наноструктур рассчитывался коэффициент отражения при нормальном падении.

**Результаты.** Благодаря тому, что диэлектрическая проницаемость неоднородных образцов была заменена общим эффективным параметром, зависящим от диэлектрической проницаемости каждого компонента, мы смогли применить теорию Друде – Лоренца для проводников в высокочастотном переменном поле и оценить параметры электронной структуры исследуемых образцов. Были рассчитаны значения плазменной и релаксационной частот для каждого образца. Это позволило оценить число свободных электронов и исследовать рассеяние в наноструктурах.

**Выводы.** Было показано, что в исследуемом диапазоне энергий в ИК-области спектра наблюдается ленгмюровская экранировка. Рассчитанные значения хорошо соотносятся с экспериментальными данными.

**Ключевые слова:** магниторефрактивный эффект, гигантское магнитосопротивление, ферромагнетик, наноструктуры

• Поступила: 09.07.2023 • Доработана: 06.10.2023 • Принята к опубликованию: 12.02.2024

**Для цитирования:** Юрасов А.Н., Сайфулина Д.А., Бахвалова Т.Н. Магниторефрактивный эффект в металлических наноструктурах Co/Pt. *Russ. Technol. J.* 2024; 12(2):57–66. <https://doi.org/10.32362/2500-316X-2024-12-2-57-66>

**Прозрачность финансовой деятельности:** Авторы не имеют финансовой заинтересованности в представленных материалах или методах.

Авторы заявляют об отсутствии конфликта интересов.

## INTRODUCTION

Heterogeneous metallic magnetic materials exhibit a giant magnetoresistance effect (GMR), associated with a change in the conductivity of the nanostructure, and depending on the mutual location of the magnetic moment vectors of the ferromagnetic regions. Such a change in the properties of matter must inevitably have an optical response correlated with the GMR. Such an effect, called the magnetorefractive effect (MRE), can indeed be observed in metallic nanostructures and consists of a change in the reflection, transmission, and absorption coefficients of an electromagnetic wave under the influence of a magnetic field [1–4]. This is based on spin-dependent scattering, as well as on the GMR effect. As a rule, magneto-optical effects are related to a change in the non-diagonal component of the dielectric permittivity tensor (DPT) under the action of a magnetic field. However, the MRE is an exception in this respect, since it is not a direct consequence of the effect of a magnetic field on a substance. It is not directly caused by the spin-orbit interaction, but is even in magnetization and is associated primarily with the diagonal part of the DPT and magnetoresistance [5, 6].

## METHODOLOGY AND STUDIED STRUCTURES

Co/Pt nanostructures [7–9] with a different volume concentration of cobalt were chosen for the MRE study. Platinum in pure form is a classical paramagnetic with a high level of stability of properties and temperature stability. It also possesses environmental inertness, corrosion resistance and good optical and conducting properties. In turn, cobalt is one of the most important ferromagnetics with significant spontaneous magnetization and a relatively high Curie temperature. This element finds broad practical application due to its high magneto-optical activity. Nanostructures based on cobalt and platinum have a good combination of mechanical strength, conductivity and magneto-optical properties. In addition, their fabrication process is relatively simple. As the amount of cobalt in the nanostructure increases, there is a transition from the paramagnetic state to the ferromagnetic state, the so-called concentration phase transition. This is accompanied by an increase in the conductivity of the structure. The type of magnetic ordering is usually determined using the Stoner criterion [10].

This work considers Co/Pt nanostructures with a volume concentration of cobalt from 0.3 to 0.6 in the energy range of 0.54–3.3 eV of incident electromagnetic waves. These nanostructures can be considered as quasi-uniform. It is thus reasonable to use the effective medium theory, in order to calculate their dielectric permittivity. Thus, knowing the dielectric permittivities of cobalt and

platinum, the effective medium methods can be used to calculate their total effective dielectric permittivity for all bulk concentrations. Since concentrations close to the mean are being considered, it is best to use the Bruggeman approximation (effective medium approximation) for the calculations. This model does not take into account dimensional effects and the influence of interfaces. So, the formulas [11] required modification, in order to improve the accuracy of calculations. The obtained dependencies of the real and imaginary parts of the dielectric permittivity are shown in Fig. 1.

These graphs clearly show that in the infrared (IR) region of the spectrum, the functions of the real and imaginary components of the dielectric permittivity resemble a hyperbolic dependence on frequency (Drudean character of the dependence). Within the framework of this model, the resulting samples with effective dielectric permittivity can be considered homogeneous. Moreover, they can also be considered in terms of the Drude–Lorentz conduction theory. This means that the electrons in the samples are considered a classical gas of non-interacting particles moving freely in the ion lattice with some average velocity. In this case, the frequency of collisions with the lattice and the mass of electrons do not depend on their velocity, and the collisions themselves are absolutely elastic. As can be seen from the graph in Fig. 1, this model works best in the IR region of the spectrum.

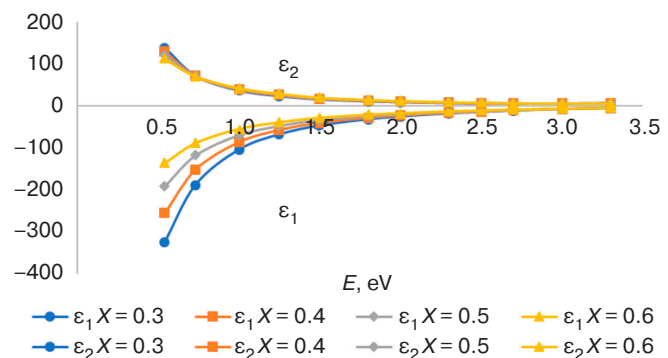


**Fig. 1.** Spectral dependencies of the real ( $\epsilon_1$ ) and imaginary ( $\epsilon_2$ ) parts of the complex dielectric permittivity for different volume concentrations of cobalt  $X$ .  $E$  is electromagnetic wave energy, eV

In this case dielectric permittivity is equal to:

$$\begin{aligned} \epsilon(\omega) = \epsilon_1 - i\epsilon_2 &= 1 - \frac{\omega_p^2}{\omega^2 + i\omega\gamma_{rel}} = 1 - \frac{\omega_p^2}{\omega} \cdot \frac{(\omega - i\gamma_{rel})}{\omega^2 + \gamma_{rel}^2} = \\ &= 1 - \frac{\omega_p^2}{\omega^2 + \gamma_{rel}^2} + i \frac{\gamma_{rel}}{\omega} \cdot \frac{\omega_p^2}{\omega^2 + \gamma_{rel}^2}, \end{aligned} \quad (1)$$

where  $\omega_p$  is the plasma frequency, and  $\gamma_{rel}$  is the relaxation frequency. These are parameters of conduction electrons characterizing the number of free electrons and their scattering.

Knowing the real part of the effective dielectric permittivity, using formula (2), the parameters of conduction electrons can be estimated. These are the effective values of the plasma  $\omega_p$  and relaxation  $\gamma_{rel}$  frequencies, as well as the relaxation time  $\tau_{rel}$  (a value inverse to the relaxation frequency) [12].

$$\frac{1}{1-\varepsilon_1} = \left( \frac{\omega}{\omega_p} \right)^2 + \left( \frac{\gamma_{rel}}{\omega_p} \right)^2. \quad (2)$$

The results of the calculations of plasma and relaxation frequencies and relaxation times are summarized in the table below.

For clarity, the dependence of the plasma frequency (in eV) on the cobalt concentration  $X$  is plotted in Fig. 2.

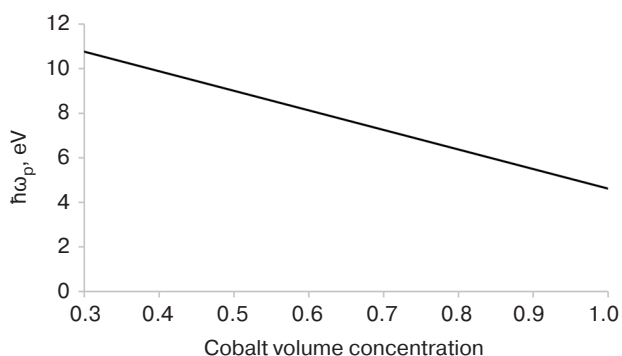


**Fig. 2.** Dependence of the plasma frequency  $\hbar\omega_p$  ( $\hbar$  is the reduced Planck constant) on the cobalt volume concentration  $X$

The calculated value of the plasma frequency of pure cobalt  $\hbar\omega_p \approx 4.46$  eV is larger than the real value of 3.69 eV. This may be due to the unaccounted influence of interzone transitions and the different contribution to the plasma frequency of electrons with spin up and spin down. The plasma frequency of pure platinum is about twice that of the plasma frequency of cobalt. This means that when the concentration of cobalt in the nanostructure increases, the plasma frequency decreases [13]. Consequently, the number of free electrons in the effective medium also decreases. The

plasma frequency from concentration varies uniformly without sharp jumps. Thus, phase transition begins at lower concentrations of cobalt, meaning that all the nanostructures under consideration have ferromagnetic order.

The electromagnetic wave range being studied herein lies between the relaxation frequency and the plasma frequency  $\gamma_{rel} < \omega < \omega_p$ . Langmuir shielding can be observed in this region. Since the radiation frequency is larger than the relaxation (collision) frequency, the field has time to change many times during the relaxation time equal to  $1/\gamma_{rel}$ . The electrons tend to compensate for the effects of the electromagnetic wave, in such a way that the field barely penetrates, although the level of attenuation is very small. Due to the reflected wave, the reflection coefficient  $R$  is close to unity. However, near the plasma frequency it decreases since the depth of Langmuir shielding begins to depend on the frequency (Fig. 3).

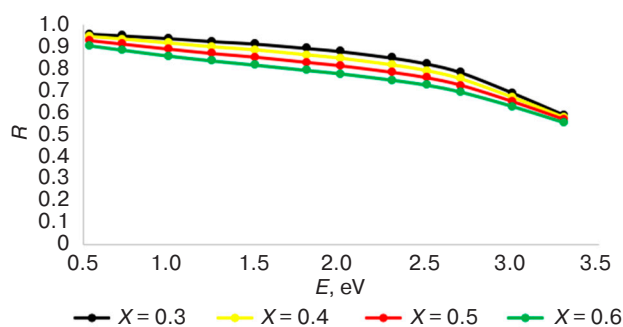


**Fig. 3.** Spectral dependencies of the reflection coefficient at normal incidence for different cobalt concentrations

The higher the cobalt concentration, the lower the reflection coefficient. In the ultraviolet (UV) region of the spectrum, the optical conductivity of the metallic nanostructure decreases significantly. This in turn affects the refraction coefficients  $n$  and extinction  $k$ , and hence the reflection coefficient  $R$ . In addition to the fact that the values of  $n$  and  $k$  are decreasing, the ratio between them also changes. In the near-IR and visible regions of the spectrum,  $k \gg n$ , but also when approaching the UV region, their values gradually equalize.

**Table.** Results of plasma frequency and relaxation time calculations

$X$	$\left( \frac{1}{\omega_p} \right)^2, \frac{1}{s^2}$	$\omega_p \cdot 10^{16}, \frac{1}{s}$	$\left( \frac{\gamma_{rel}}{\omega_p} \right)^2, \frac{1}{s^2}$	$\gamma_{rel} \cdot 10^{16}, \frac{1}{s}$	$\tau_{rel} \cdot 10^{-16}, s$
0.3	$0.39 \cdot 10^{-32}$	1.60	0.001	0.04	27.87
0.4	$0.45 \cdot 10^{-32}$	1.49	0.001	0.05	21.19
0.5	$0.52 \cdot 10^{-32}$	1.38	0.002	0.06	16.57
0.6	$0.61 \cdot 10^{-32}$	1.28	0.004	0.07	13.00

The real and imaginary parts of dielectric permittivity are equal to:

$$\varepsilon_1(\omega) = n^2 - k^2, \quad (3)$$

$$\varepsilon_2(\omega) = 2nk. \quad (4)$$

Optical conductivity  $\sigma_{\text{opt}}$  is equal to:

$$\sigma_{\text{opt}}(\omega) = \frac{Ne^2}{m\gamma_{\text{rel}} \left( 1 + \left( \frac{\omega}{\gamma_{\text{rel}}} \right)^2 \right)^2} = \frac{1}{\rho}, \quad (5)$$

where  $m$  is the mass of an electron,  $N$  is the number of electrons,  $e$  is the charge of an electron,  $\rho$  is the electrical resistance.

The imaginary part of the diagonal component  $\text{Im } \varepsilon$  of the DPT is related to the optical conductivity of the metal  $\sigma_{\text{opt}}$ :

$$\sigma_{\text{opt}}(\omega) = \frac{\omega}{4\pi} \text{Im } \varepsilon(\omega) = \frac{\omega}{2\pi} nk. \quad (6)$$

When an alloy with GMR is magnetized, the optical conductivity changes in accordance with the change in magnetoresistance. The change in optical conductivity can be expressed through the magnetoresistive effect [14]:

$$\sigma_{\text{opt}}(\omega) = \frac{1}{\rho_0} - \frac{1}{\rho_H} = \frac{\Delta\rho}{\rho_0^2 \left( 1 - \frac{\Delta\rho}{\rho_0} \right)} = \frac{\frac{\Delta\rho}{\rho_0}}{\left( 1 - \frac{\Delta\rho}{\rho_0} \right)} \sigma, \quad (7)$$

where  $\Delta\sigma_{\text{opt}}$  is the magnetic conductivity,  $\rho_H$  is the electrical resistance in a magnetic field,  $\rho_0$  is the electrical resistance without a magnetic field, and  $\Delta\rho/\rho_0$  is the magnetoresistance of the material.

Using formulas (3), (4), and (6) in a magnetic field, by replacing the refraction and extinction coefficients by  $n_H = n + \Delta n$  and  $k_H = k + \Delta k$ , we can calculate  $\Delta n$  and  $\Delta k$  through  $\Delta\sigma_{\text{opt}}$ . In this case, the product  $\Delta n \cdot \Delta k$  can be neglected as a value of the second order of smallness.

$$\Delta n = \frac{2\pi\Delta\sigma}{\omega} \left( \frac{n+k}{n^2+k^2} \right), \quad (8)$$

$$\Delta k = \frac{2\pi\Delta\sigma}{\omega} \left( \frac{n-k}{n^2+k^2} \right). \quad (9)$$

Thus, considering formulas (7)–(9), the MRE can be estimated using optical parameters and magnetoresistive effect parameter [11].

MRE on reflection at normal incidence is calculated using the following formula:

$$\frac{\Delta R}{R} = \frac{R_0 - R_H}{R_0}, \quad (10)$$

where  $R_H$  and  $R_0$  are the light reflection coefficients of the sample in the magnetic field and without the field, respectively.

## MAIN RESULTS AND DISCUSSION

In Fig. 4, the spectral dependencies of the MRE parameter at different cobalt concentrations for the magnetoresistive effect  $\frac{\Delta\rho}{\rho} = 1\%, 5\%, 10\%$  are plotted.

MRE has a negative value. This means that the reflection coefficient of the nanostructure increases in the magnetic field. The effect is more noticeable the larger the magnetoresistive effect and the higher the cobalt concentration. This means that the MRE is very sensitive to changes in the microstructure, which affects its conductivity. The MRE parameter takes the highest value in the low frequency region close to the relaxation frequency [15–18].

Now let us calculate the MRE parameter at an arbitrary angle of incidence using the  $30^\circ$  angle as an example, using the Fresnel equations for s-polarization. Let us represent the nanostructures under consideration as films deposited on a silicon substrate. Then the samples can be considered as three-layer air-Co/Pt-Si structures.

This model will be closer to real samples on a silicon substrate. The reflection coefficient of the s-component for the whole three-layer structure  $jki$  is equal to [17]:

$$R_s = \left| \frac{r_{jk} + F_k^2 r_{ki}}{1 + F_k^2 r_{jk} r_{ki}} \right|^2, \quad (11)$$

where  $F_k = e^{\frac{-2\pi g_k d_k}{\lambda}}$  is the phase multiplier in the  $k$ th layer,  $g_i = \sqrt{n_j^2 - n_i^2 \sin^2 \varphi}$  is the parameter for convenient calculation of reflection coefficients at the

interfaces,  $r_{jk} = \frac{g_j n_j^2 - g_k n_k^2}{g_j n_j^2 + g_k n_k^2}$  is the partial reflection and transmission coefficient at the interface of  $j$ – $k$  media,  $\varphi$  is the angle of incidence of light from the first medium, and  $d_k$  is the thickness of the corresponding medium.

In Fig. 5, the spectral dependencies of the MRE parameter with regard to the angle of incidence, substrate influence and thickness at different cobalt concentrations for the magnetoresistive effect are plotted:  $\frac{\Delta\rho}{\rho} = 1\%, 5\%, 10\%$ .



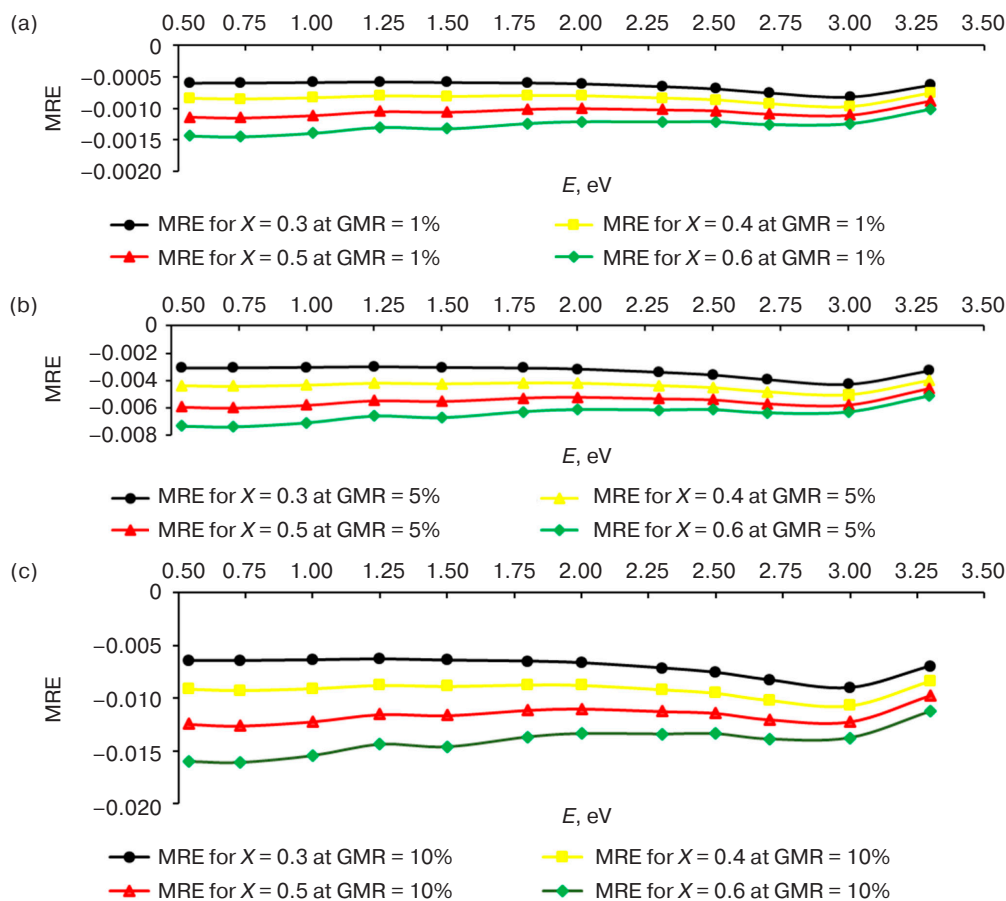


**Fig. 4.** MRE spectral dependencies for different cobalt concentrations at different GMR values: (a) 1%, (b) 5%, (c) 10%

Experimental data of the MRE parameter for the Si/Ta(2)/Co<sub>50</sub>Pt<sub>50</sub>(4.6)/Ta(2) nanostructure, where Ta is the buffer layer (Fig. 6), are plotted for comparison in the graphs (Fig. 5). The experimental curve lies roughly between the plots for  $X = 0.5$  and  $X = 0.6$  at GMR = 5%. It is worth considering that the thickness of the  $k$ th layer

has a noticeable effect on the MRE parameter, since it is under the exponent function. As can be seen from the graph in Fig. 5, the MRE parameter in the IR region of the spectrum increases sharply up to some maximum value. It then gradually decreases. The greater the cobalt concentration, the more strongly this maximum point

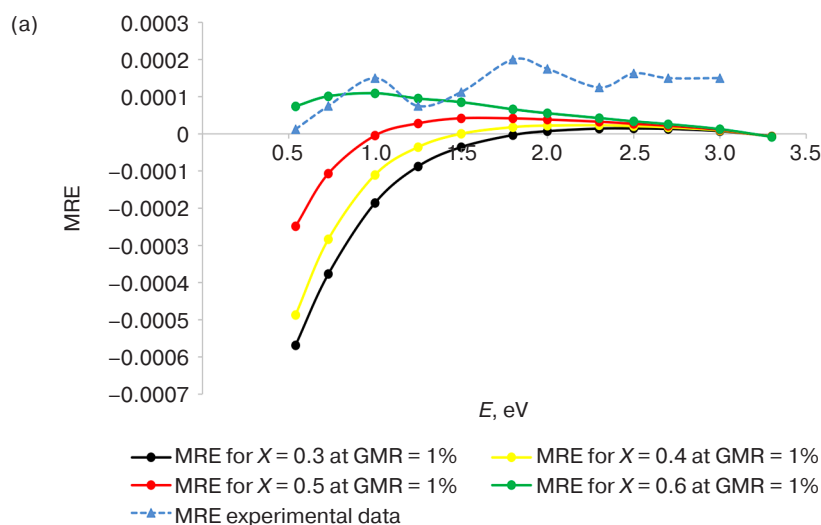


**Fig. 5 (start).** MRE spectral dependencies for different cobalt concentrations at different GMR values for s-polarization and 30° angle of incidence calculated by Fresnel formulas and experimental data for s-polarization, 30° angle of incidence: (a) GMR = 1%, (b) GMR = 5%, (c) GMR = 10%

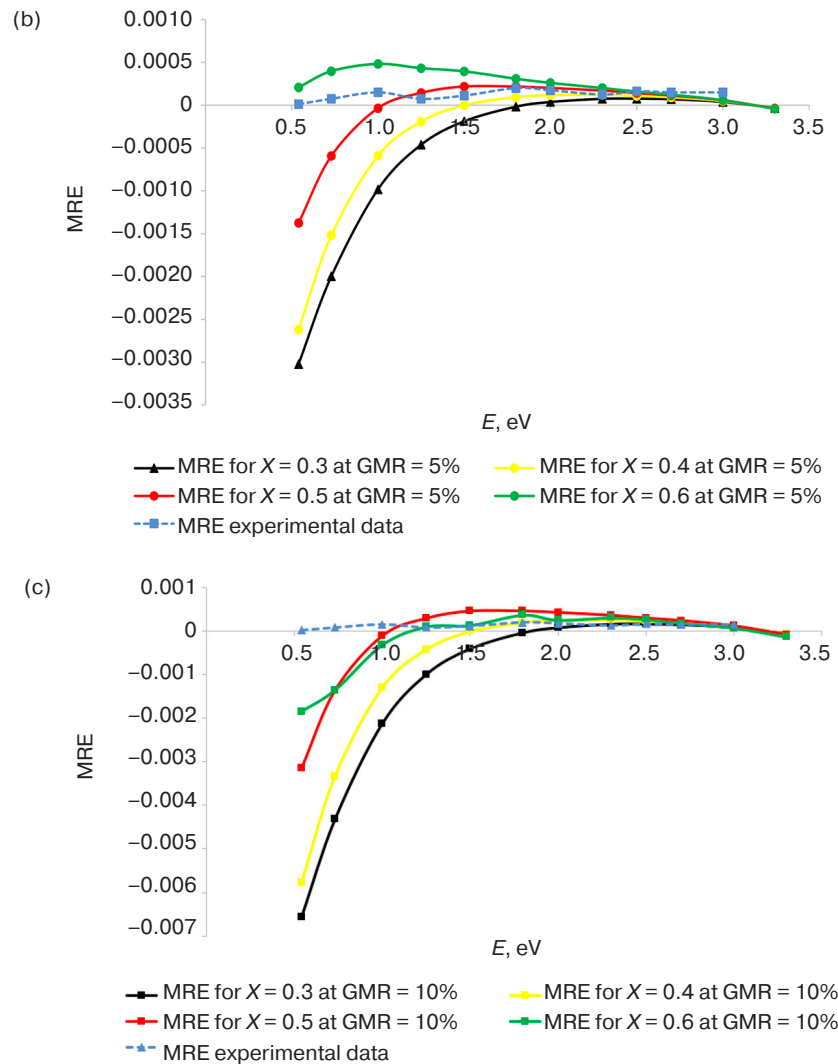


**Fig. 5 (end).** MRE spectral dependencies for different cobalt concentrations at different GMR values for s-polarization and  $30^\circ$  angle of incidence calculated by Fresnel formulas and experimental data for s-polarization,  $30^\circ$  angle of incidence: (a) GMR = 1%, (b) GMR = 5%, (c) GMR = 10%

is shifted towards the IR range. At the same time, the greater the concentration of cobalt and HMS, the more pronounced the oscillations of the MRE parameter. The sign of the effect parameter changes. This means that after some value of the emission frequency, the reflection coefficient in the magnetic field decreases. At GMR 10%, the MRE parameter for cobalt concentration 0.5 at some frequencies slightly exceeds the MRE parameter for concentration 0.6.

At high frequencies, the concentration of cobalt has practically no effect on the MRE, which itself is very small. This correlates well with the data in Fig. 1. The values of the real and imaginary components of the dielectric permittivity for all samples also converge at high frequencies. At an electromagnetic wave energy of about 2 eV, there is no special difference between samples with  $X = 0.3$  and 0.6. This does not coincide with the experimental data, since the experimental curve at high frequencies on the contrary increases. This is

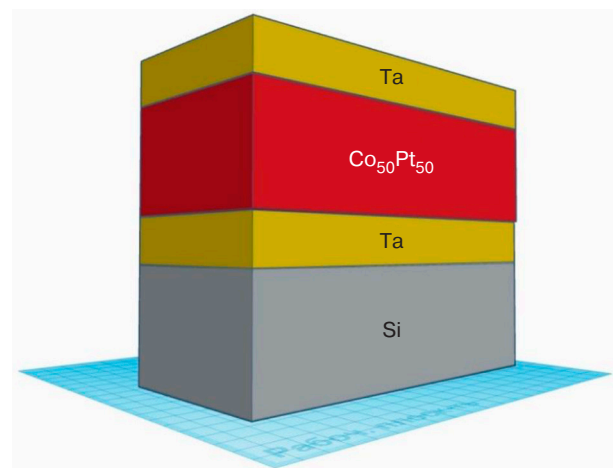


**Fig. 6.** Schematic representation of heterogeneous layered Si/Ta(2)/Co<sub>50</sub>Pt<sub>50</sub>(4.6)/Ta(2) nanostructure

because the model considered herein does not describe the effects at high frequencies. All calculations are based on the dielectric permittivity of the nanostructure. Thus, when refining the model, it will be necessary to calculate more accurately the dielectric permittivity of the considered nanostructures at high frequencies [18].

It can be concluded that the model under consideration is best suited for calculating spectra in the IR region. However, it does not take into account the influence of interzone transitions and size effects. The MRE strongly depends on the GMR. The higher the cobalt concentration, the more noticeable this dependence is. This means that it is very sensitive to the microstructure of the sample. The graph in Fig. 5c, it shows the oscillatory character of the dependence of the MRE parameter for the nanostructure with  $X = 0.6$ . Moreover, unlike the previous graphs, it shows the intersection of the curves with  $X = 0.5$  and  $0.6$  in the IR region of the spectrum. At some frequencies the curve  $0.5$  is higher than the curve  $0.6$ .

## CONCLUSIONS

This study investigates plasma frequencies, reflection coefficients, and MRE spectra on reflection at normal incidence. The MRE spectra for Co/Pt nanostructures with different cobalt concentrations at an angle of incidence of  $30^\circ$  for s-polarization were

calculated. The data obtained for a  $30^\circ$  incidence angle was compared with the experimental data, and a good level of agreement was established. A complete correlation between the MRE and magnetoresistance was explicitly shown. The effect is more noticeable the larger the magnetoresistivity and the higher the cobalt concentration. This means that the MRE is very sensitive to microstructure changes affecting its conductivity. The highest value of the MRE parameter is in the low frequency region, close to the relaxation frequency.

## ACKNOWLEDGMENTS

The work was implemented in the scientific structural subdivision "Laboratory of New Functional Materials" of RTU MIREA under the grant FSFZ-2022-0007 of the Ministry of Education and Science of the Russian Federation and with the support of the Ministry of Education and Science of the Russian Federation (State task for universities No. FGFZ-2023-0005).

### Authors' contributions

**A.N. Yurasov**—setting the aims and objectives of the study, discussing and summarizing the results, and drawing conclusions.

**D.A. Sayfullina**—calculation of the magnetorefractive effect and plotting.

**T.N. Bakhvalova**—developing the theory of the magnetorefractive effect.

## REFERENCES

1. Granovsky A., Sukhorukov Yu., Gan'shina E., Telegin A. Magnetorefractive effect in magnetoresistive materials. In: *Magnetophotonics: From Theory to Applications*. Berlin Heidelberg: Springer; 2013. P. 107–133. [http://doi.org/10.1007/978-3-642-35509-7\\_5](http://doi.org/10.1007/978-3-642-35509-7_5)
2. Shkurdoda Yu.O., Dekhtyaruk L.V., Basov A.G., Chornous A.M., Shabelnyk Yu.M., Kharchenko A.P., Shabelnyk T.M. The giant magnetoresistance effect in Co/Cu/Co three-layer films. *J. Magn. Magn. Mater.* 2019;477:88–91. <https://doi.org/10.1016/j.jmmm.2019.01.040>
3. Dekhtyaruk L.V., Kharchenko A.P., Klymenko Yu.O., Shkurdoda Yu.O., Shabelnyk Yu.M., Bezdidko O.V., Chornous A.M. Negative and Positive Effect of Giant Magnetoresistance in The Magnetically Ordered Sandwich. In: *2020 IEEE 10th International Conference Nanomaterials: Applications & Properties (NAP)*. 2020. P. 01NMM13-1–01NMM13-3. <https://doi.org/10.1109/NAP51477.2020.9309694>
4. Kelley C.S., Naughton J., Benson E., Bradley R.C., Lazarov V.K., Thompson S.M., Matthew J.A. Investigating the magnetic field-dependent conductivity in magnetite thin films by modelling the magnetorefractive effect. *J. Phys.: Condens. Matter.* 2014;26(3):036002. <http://doi.org/10.1088/0953-8984/26/3/036002>
5. Lysina E.A., Yurasov A.N. Magneto-optical effects in CoSiO<sub>2</sub> nanocomposite. In: *Informatika i tekhnologii. Innovatsionnyye tekhnologii v promyshlennosti i informatike (MNTK FTI 2017) (Informatics and Technologies. Innovative Technologies in Industry and Informatics)*. Moscow: MIREA; 2017. P. 622–628 (in Russ.).
6. Lobov I.D., Kirillova M.M., Makhnev A.A., et al. Magneto-optical, optical, and magnetotransport properties of Co/Cu superlattices with ultrathin cobalt layers. *Phys. Solid State.* 2017;59(1):53–62. <https://doi.org/10.1134/S1063783417010206> [Original Russian Text: Lobov I. D. Kirillova M.M., Makhnev A.A., Romashev L.N., Korolev A.V., Milyaev M.A., Proglyado V.V., Bannikova N.S., Ustinov V.V. Magneto-optical, optical, and magnetotransport properties of Co/Cu superlattices with ultrathin cobalt layers. *Fizika Tverdogo Tela.* 2017;59(1):54–62 (in Russ.). <https://doi.org/10.21883/FTT.2017.01.43950.161>]
7. Oh J., Humbard L., Humbert V., Sklenar J., Mason N. Angular evolution of thickness-related unidirectional magnetoresistance in Co/Pt multilayers. *AIP Advances.* 2019;9(4):045016. <https://doi.org/10.1063/1.5079894>
8. Kawaguchi M., Towa D., Lau Y.-C., Takahashi S., Hayashi M. Anomalous spin Hall magnetoresistance in Pt/Co bilayers. *Appl. Phys. Lett.* 2018;112(20):202405. <https://doi.org/10.1063/1.5021510>



9. Heigl M., Wendler R., Haugg S.D., Albrecht M. Magnetic properties of Co/Ni-based multilayers with Pd and Pt insertion layers. *J. Appl. Phys.* 2020;127(23):233902. <https://doi.org/10.1063/5.0010112>
10. Povzner A.A., Volkov A.G., Filanovich A.N. Electronic structure and magnetic susceptibility of nearly magnetic metals (palladium and platinum). *Phys. Solid State.* 2010;52(10):2012–2018. <https://doi.org/10.1134/S1063783410100021> [Original Russian Text: Povzner A.A., Volkov A.G., Filanovich A.N. Electronic structure and magnetic susceptibility of nearly magnetic metals (palladium and platinum). *Fizika Tverdogo Tela.* 2010;52(10):1879–1884 (in Russ.).]
11. Yurasov A.N., Telegin A.V., Bannikova N.S., et al. Features of Magnetorefractive Effect in a  $[\text{CoFe/Cu}]_n$  Multilayer Metallic Nanostructure. *Phys. Solid State.* 2018;60(2):281–287. <https://doi.org/10.1134/S1063783418020300> [Original Russian Text: Yurasov A.N., Telegin A.V., Bannikova N.S., Milyaev M.A., Sukhorukov Yu.P. Features of Magnetorefractive Effect in a  $[\text{CoFe/Cu}]_n$  Multilayer Metallic Nanostructure. *Fizika Tverdogo Tela.* 2018;60(2):276–282 (in Russ.). <https://doi.org/10.21883/FTT.2018.02.45381.201>]
12. Lobov I.D., Kirillova M.M., Romashev L.N., et al. Magnetorefractive effect and giant magnetoresistance in  $\text{Fe}(t_x)/\text{Cr}$  superlattices. *Phys. Solid State.* 2009;51(12):2480–2485. <https://doi.org/10.1134/S1063783409120099> [Original Russian Text: Lobov I.D., Kirillova M.M., Romashev L.N., Milyaev M.A., Ustinov V.V. Magnetorefractive effect and giant magnetoresistance in  $\text{Fe}(t_x)/\text{Cr}$  superlattices. *Fizika Tverdogo Tela.* 2009;51(12):2337–2341 (in Russ.).]
13. Pogodaeva M.K., Levchenko S.V., Drachev V.P., Gabitov I.R. Optical properties of metals from the first principles. *Photon Express.* 2021;6(174):294–295 (in Russ.).
14. Ustinov V.V., Sukhorukov Yu.P., Milyaev M.A., et al. Magnetotransmission and magnetoreflexion in multilayer FeCr nanostructures. *J. Exp. Theor. Phys.* 2009;108(2):260–266. <https://doi.org/10.1134/S1063776109020083> [Original Russian Text: Ustinov V.V., Sukhorukov Yu.P., Milyaev M.A., Granovskii A.B., Yurasov A.N., Gan'shina E.A., Telegin A.V. Magnetotransmission and magnetoreflexion in multilayer FeCr nanostructures. *Zhurnal Eksperimental'noi i Teoreticheskoi Fiziki.* 2009;135(2):293–300 (in Russ.).]
15. Jacquet J.C., Valet T. A new magneto-optical effect discovered on magnetic multilayers: The magnetorefractive effect. *MRS Online Proceedings Library (OPL).* 1995;384:477–490. <https://www.doi.org/10.1557/PROC-384-477>
16. Kravets V.G. Correlation between the magnetoresistance, IR magnetoreflexance, and spin-dependent characteristics of multilayer magnetic films. *Phys. Res. Int.* 2012;2012(5):323279. <https://www.doi.org/10.1155/2012/323279>
17. Maevskii V.M. Theory of magneto-optical effects in multilayer systems with arbitrary orientation of magnetization. *Fizika metallov i metallovedenie = Physics of Metals and Metallography.* 1985;59:213–216 (in Russ.).
18. Yurasov A.N. Magnetorefractive effect in nanostructures. *Pribory = Instruments.* 2022;4(262):22–25 (in Russ.).

## СПИСОК ЛИТЕРАТУРЫ

1. Granovsky A., Sukhorukov Yu., Gan'shina E., Telegin A. Magnetorefractive effect in magnetoresistive materials. In: *Magnetophotonics: From Theory to Applications*. Berlin Heidelberg: Springer; 2013. P. 107–133. [http://doi.org/10.1007/978-3-642-35509-7\\_5](http://doi.org/10.1007/978-3-642-35509-7_5)
2. Shkurdoda Yu.O., Dekhtyaruk L.V., Basov A.G., Chornous A.M., Shabelnyk Yu.M., Kharchenko A.P., Shabelnyk T.M. The giant magnetoresistance effect in Co/Cu/Co three-layer films. *J. Magn. Magn. Mater.* 2019;477:88–91. <https://doi.org/10.1016/j.jmmm.2019.01.040>
3. Dekhtyaruk L.V., Kharchenko A.P., Klymenko Yu.O., Shkurdoda Yu.O., Shabelnyk Yu.M., Bezdidko O.V., Chornous A.M. Negative and Positive Effect of Giant Magnetoresistance in The Magnetically Ordered Sandwich. In: *2020 IEEE 10th International Conference Nanomaterials: Applications & Properties (NAP)*. 2020. P. 01NMM13-1–01NMM13-3. <https://doi.org/10.1109/NAP51477.2020.9309694>
4. Kelley C.S., Naughton J., Benson E., Bradley R.C., Lazarov V.K., Thompson S.M., Matthew J.A. Investigating the magnetic field-dependent conductivity in magnetite thin films by modelling the magnetorefractive effect. *J. Phys.: Condens. Matter.* 2014;26(3):036002. <http://doi.org/10.1088/0953-8984/26/3/036002>
5. Лысина Е.А., Юрасов А.Н. Магнитооптические эффекты в нанокompозите  $\text{CoSiO}_2$ . *Информатика и технологии. Инновационные технологии в промышленности и информатике (МНТК ФТИ – 2017)*. М.: МИРЭА; 2017. С. 622–628.
6. Лобов И.Д., Кириллова М.М., Махнев А.А., Ромашев Л.Н., Королев А.В., Мильяев М.А., Проглядо В.В., Банникова Н.С., Устинов В.В. Магнитооптические, оптические и магнитотранспортные свойства сверхрешеток Co/Cu с ультратонкими слоями кобальта. *Физика твердого тела.* 2017;59(1):54–62. <https://doi.org/10.21883/FTT.2017.01.43950.161>
7. Oh J., Humbard L., Humbert V., Sklenar J., Mason N. Angular evolution of thickness-related unidirectional magnetoresistance in Co/Pt multilayers. *AIP Advances.* 2019;9(4):045016. <https://doi.org/10.1063/1.5079894>
8. Kawaguchi M., Towa D., Lau Y.-C., Takahashi S., Hayashi M. Anomalous spin Hall magnetoresistance in Pt/Co bilayers. *Appl. Phys. Lett.* 2018;112(20):202405. <https://doi.org/10.1063/1.5021510>
9. Heigl M., Wendler R., Haugg S.D., Albrecht M. Magnetic properties of Co/Ni-based multilayers with Pd and Pt insertion layers. *J. Appl. Phys.* 2020;127(23):233902. <https://doi.org/10.1063/5.0010112>
10. Повзнер А.А., Волков А.Г., Филанович А.Н. Электронная структура и магнитная восприимчивость почти магнитных металлов (на примере палладия и платины). *Физика твердого тела.* 2010;52(10):1879–1884.
11. Юрасов А.Н., Телегин А.В., Банникова Н.С., Мильяев М.А., Сухоруков Ю.П. Особенности магниторефрактивного эффекта в многослойной металлической наноструктуре  $[\text{CoFe/Cu}]_n$ . *Физика твердого тела.* 2018;60(2):276–282. <https://doi.org/10.21883/FTT.2018.02.45381.201>

12. Лобов И.Д., Кириллова М.М., Ромашев Л.Н., Миляев М.А., Устинов В.В. Магниторефрактивный эффект и гигантское магнитосопротивление в сверхрешетках  $\text{Fe}(t_x)/\text{Cr}$ . *Физика твердого тела*. 2009;51(12):2337–2341.
13. Погодаева М.К., Левченко С.В., Драчев В.П., Габитов И.Р. Оптические свойства металлов из первых принципов. *Фотон-экспресс*. 2021;6(174):294–295. <https://doi.org/10.24412/2308-6920-2021-6-294-295>
14. Устинов В.В., Сухоруков Ю.П., Миляев М.А., Грановский А.Б., Юрасов А.Н., Ганьшина Е.А., Телегин А.В. Магнитопропускание и магнитоотражение в многослойных наноструктурах  $\text{FeCr}$ . *Журнал экспериментальной и теоретической физики*. 2009;135(2):293–300.
15. Jacquet J.C., Valet T. A new magneto-optical effect discovered on magnetic multilayers: The magnetorefractive effect. *MRS Online Proceedings Library (OPL)*. 1995;384:477–490. <https://www.doi.org/10.1557/PROC-384-477>
16. Kravets V.G. Correlation between the magnetoresistance, IR magnetorefractance, and spin-dependent characteristics of multilayer magnetic films. *Phys. Res. Int.* 2012;2012(5):323279. <https://www.doi.org/10.1155/2012/323279>
17. Маевский В.М. Теория магнитооптических эффектов в многослойных системах с произвольной ориентацией намагниченности. *Физика металлов и металловедение*. 1985;59:213–216.
18. Юрасов А.Н. Магниторефрактивный эффект в наноструктурах. *Приборы*. 2022;4(262):22–25.

#### About the authors

**Alexey N. Yurasov**, Dr. Sci. (Phys.-Math.), Professor, Department of Nanoelectronics, Institute for Advanced Technologies and Industrial Programming, MIREA – Russian Technological University (78, Vernadskogo pr., Moscow, 119454 Russia). E-mail: alexey\_yurasov@mail.ru. ResearcherID M-3113-2016, Scopus Authors ID 6602974416, RSCI SPIN-code 4259-8885, <https://orcid.org/0000-0002-9104-3529>

**Diana A. Sayfullina**, Student, Institute for Advanced Technologies and Industrial Programming, MIREA – Russian Technological University (78, Vernadskogo pr., Moscow, 119454 Russia). E-mail: diana-sayfullina@mail.ru. ResearcherID IQU-6785-2023, RSCI SPIN-code 4397-9205, <https://orcid.org/0009-0006-2905-9753>

**Tatiana N. Bakhvalova**, Teacher, Department of Nanoelectronics, Institute for Advanced Technologies and Industrial Programming, MIREA – Russian Technological University (78, Vernadskogo pr., Moscow, 119454 Russia). E-mail: bahvalova@mirea.ru. ResearcherID ITW-2747-2023, Scopus Author ID 35145196400, <https://orcid.org/0000-0001-7595-785X>

#### Об авторах

**Юрасов Алексей Николаевич**, д.ф.-м.н., профессор, профессор кафедры нанoeлектроники, Институт перспективных технологий и индустриального программирования ФГБОУ ВО «МИРЭА – Российский технологический университет» (119454, Россия, Москва, пр-т Вернадского, д. 78). E-mail: alexey\_yurasov@mail.ru. ResearcherID M-3113-2016, Scopus Authors ID 6602974416, SPIN-код РИНЦ 4259-8885, <https://orcid.org/0000-0002-9104-3529>

**Сайфулина Диана Алексеевна**, студент, Институт перспективных технологий и индустриального программирования ФГБОУ ВО «МИРЭА – Российский технологический университет» (119454, Россия, Москва, пр-т Вернадского, д. 78). E-mail: diana-sayfullina@mail.ru. ResearcherID IQU-6785-2023, SPIN-код РИНЦ 4397-9205, <https://orcid.org/0009-0006-2905-9753>

**Бахвалова Татьяна Николаевна**, преподаватель, кафедра нанoeлектроники, Институт перспективных технологий и индустриального программирования ФГБОУ ВО «МИРЭА – Российский технологический университет» (119454, Россия, Москва, пр-т Вернадского, д. 78). E-mail: bahvalova@mirea.ru. ResearcherID ITW-2747-2023, Scopus Author ID 35145196400, <https://orcid.org/0000-0001-7595-785X>

*Translated from Russian into English by Lyudmila O. Bychkova*

*Edited for English language and spelling by Dr. David Mossop*